Engineering Structures 303 (2024) 117489

Contents lists available at ScienceDirect

Engineering Structures

journal homepage: www.elsevier.com/locate/engstruct

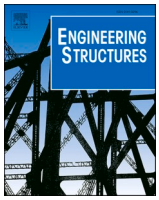

Numerical investigation on the behaviour of socket connections in GFRP-reinforced precast concrete

Mohamed H. El-Naqeeb [a,b,1], Reza Hassanli [a,*,2], Yan Zhuge [a,3], Xing Ma [a,4], Allan Manalo [c,5]

[a] University of South Australia, UniSA STEM, Mawson Lakes, SA 5095, Australia
[b] Badr University in Cairo, School of Engineering and Technology, Cairo 11829, Egypt
[c] Center for Future Materials, School of Engineering, University of Southern Queensland, QLD 4350, Australia

ARTICLE INFO

Keywords:
Finite element analysis
GFRP
Numerical simulation
Socket connection
Precast concrete

ABSTRACT

Precast socket connections involve connecting precast columns and beams through prefabricated pockets. This method is widely used in the precast concrete industry due to its ability to accelerate construction and provide strong connections. To enhance their benefits and ensure durability in harsh environments, noncorrodible Glass Fibre Reinforced Polymers (GFRP) reinforcement is commonly employed as an effective reinforcement solution. The current numerical study investigates the performance of GFRP precast socket connections using epoxy resin for assembly. Finite element models were developed and verified against the experimental results of three specimens. The numerical model was then employed to investigate the influence of several key parameters influencing the behaviour of precast GFRP socket connections. It was found that the performance of the connection depends on the socket depth, concrete depth under the socket, size of the beam, and socket-filling material. Additionally, the stiffness and capacity of the connection were found to be strongly affected by the column reinforcement ratio. The study reveals that the maximum capacity of the connection can be achieved using a socket depth equal to 1.4 times the thickness of the column. Moreover, the socket region should be properly confined by concrete of thickness at least 0.8 of the column thickness at the overhanging side of the beam and 0.5 times the column width in the transverse direction as well as the bottom of the socket, to ensure the development of the full capacity at the connection. Although epoxy resin has many advantages, including non-shrinkage, high workability, and high strength, it was found that replacing the epoxy resin with ultra-high-performance concrete improves the connection performance, and hence the required depth of the socket can be reduced. The results of this study can be used to safely work out the minimum size and detailing of the GFRP-RC socket connections using epoxy resin for assembly.

1. Introduction

In recent decades, precast concrete has been widely utilized in the construction of numerous bridges, marine infrastructures and buildings, owing to its unique advantages including fast construction, enhanced productivity, superior material quality, and increased site safety by reducing the number of labourers required in the field. Precast concrete is also used as part of Accelerated Bridge Construction (ABC), which helps minimize the impact on traffic and road functionality during construction [1], and hence significantly reduces the associated costs. A precast concrete structure is an assembly of precast beams and columns connected at the construction site. The method of connection used for assembly can significantly impact the structure's performance and the flexibility of the connection in transferring moments between the beam and column [2].

Connections in precast concrete structures can be classified as pin, rigid, and semi-rigid connections. Pin connections do not allow for the transfer of moment between members, while proper rigid (moment-

* Corresponding author.
E-mail address: reza.hassanli@unisa.edu.au (R. Hassanli).
[1] ORCID: https://orcid.org/0000-0002-0573-2978
[2] ORCID: https://orcid.org/0000-0001-5855-6405
[3] ORCID: http://orcid.org/0000-0003-1620-6743
[4] ORCID: http://orcid.org/0000-0001-5488-5252
[5] ORCID: https://orcid.org/0000-0003-0493-433X

https://doi.org/10.1016/j.engstruct.2024.117489
Received 9 July 2023; Received in revised form 22 December 2023; Accepted 5 January 2024
Available online 13 January 2024

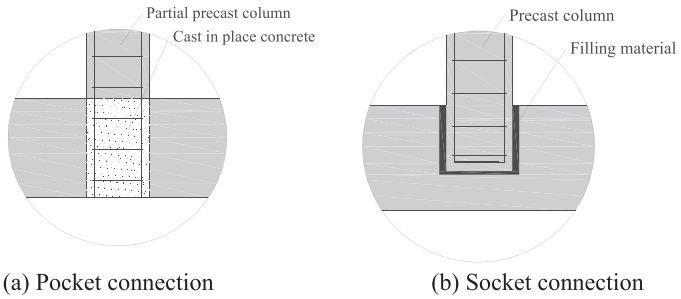

Fig. 1. Pocket and socket connections.

resisting) connections are crucial for an effective load transferring mechanism between beams and columns, particularly when lateral loads are applied [2]. Different connection systems have been developed previously, including grout sleeve [3], grout duct [4], pocket [5], socket connections [6], and prestressed tendons [7]. The high-strength properties of prestressed tendons enable effective energy dissipation and self-centring of the column following cyclic loading [7]. However, the efficiency of this method can be affected by tendon relaxation. Grout sleeve connections can effectively connect the reinforcement between precast members [8], but the relative stiffness between the column and beam [9], the type of grout used, and defects in grouting [3] can impact its efficiency. Grout duct connections require the passing of reinforcement between two elements through a prefabricated duct and filling with grout to ensure connection integrity [4]. From a construction perspective, pocket and socket connections are regarded as simple methods for connecting beams to columns or columns to foundations. This is achieved by creating a pocket in the beam or foundation and filling it with bonding material [5]. These connections reduce the need for precise alignment or adjustments typically required with grout ducts and post-tensioning, consequently lowering the risk of installation errors. Socket connections also require less labour-intensive procedures compared to the intricate grouting process, where grout defects can impact connection performance, or the tensioning of cables, where force relaxation can affect the performance. Both connection types exhibit similarities as they involve creating a pocket in the beam or foundation. However, their execution differs. In a pocket connection, the reinforcement of columns passes through the pocket, which is later filled with cast-in-place concrete. Conversely, a socket connection entails filling the space between the column and the socket wall with connecting materials like grout or epoxy (see Fig. 1).

The performance of pocket and socket connections was experimentally addressed in previous studies. It has been reported that the capacity of these types of connections depends on the socket depth (column embedded depth), the roughness of the socket surface, the strength of filling material, and the gap size between the column and socket wall [6]. Sufficient socket depth is essential to ensure well integrity of the structure and the development of plastic hinge at the columns [10] while oversized socket depth requires larger foundation depth and material causing additional costs. Han et al. [11] evaluated the cyclic performance of smooth surface socket connections with socket depth equal to 0.5, 1.0, and 1.5 of the column diameter using high strength grout. It was found that the performance of connection with embedded depth not less than 1.0 of the column diameters was similar to the cast-in-place connection. However, the energy dissipation and ductility were significantly improved in the case of embedded depth equal to 1.5 of the column diameter. An embedded depth equal to 1.1 of the column thickness was found sufficient to attain the connection capacity [5]. In another study, the socket connection with an embedded depth equal to 0.8 of the column diameter and using tooth shaped shear key socket filled with ultra-high performance concrete showed comparable behaviour to the corresponding castin-place one [12]. The socket connection with confining corrugated steel pipe and socket depth equal to 1.2 and 1.0 of the column diameter performed well where the plastic hinge was developed at the column [13,14]. Zhou et al. [15] proposed a new socket connection with outer and inner post pour concrete, novel shear keys, and a special arrangement of reinforcement for hollow column connections. It was reported that the connection performed satisfactorily with an embedded depth equal to about 0.44 of the column diameter.

The long-term performance of steel-RC structures relies on effectively protecting steel reinforcement from corrosion. In harsh environments, such as jetty structures, the high level of chlorides can cause steel reinforcement corrosion, leading to obvious structural failure and increased maintenance costs [16]. To address this challenge, non-corroding fibre reinforced polymer (FRP) reinforcement has emerged as an effective alternative to conventional steel reinforcement [17,18]. However, FRP has a comparatively lower elastic modulus and exhibits linear elastic behaviour. This results in significant differences in the performance of structures reinforced with FRP compared to steel reinforced ones [19]. Previous studies have demonstrated the feasibility of using glass FRP (GFRP) reinforcement in cast-in-place connections [20–22] and examined the influence of various parameters, including joint reinforcement, transverse beams, and slab contribution. Mady et al. [21] concluded that GFRP cast-in-place connections can be designed to satisfy both strength and deformation requirements. However, the energy dissipation of GFRP cast-in-place connections was less than that of steel-reinforced connections due to the linear elastic behaviour of GFRP bars, resulting in narrow hysteresis loops [20].

While some studies have focused on GFRP cast-in-place connections, there is limited research on GFRP precast connections. Ngo et al. [23] conducted a study on the cyclic performance of a dry precast GFRP connection using a concrete end block and GFRP bolts. It was found that the capacity of the proposed connection was superior to that of the cast-in-place connection. Recently, the cyclic performance of two large-scale GFRP precast frames with socket and connecting reinforcement in ducts was evaluated [24,25]. It was reported that the frame connected by reinforcement in ducts outperformed that with socket connections due to the premature failure of the socket connection by the use of a shallow socket of depth equal to half of the column thickness [25]. Additionally, an experimental investigation [26] was conducted to evaluate the cyclic behaviour of precast GFRP socket beam-column connections using epoxy resin as a socket material [26]. The lateral capacity of the connection with a socket depth equal to half of the column size was significantly reduced compared to that of a connection with a socket depth equal to the column thickness. Immature failure of the socket connection due to the lack of concrete material around the socket area as well as the low elasticity of epoxy material used in the socket area, has also been reported [26].

Although extensive research on steel reinforced socket connections suggested that a socket of depth less than 1.0 of the column thickness is sufficient to ensure the development of connection full capacity [11,14], the previous study on GFRP socket connection with a socket depth equal to the column size indicated that the connection suffered premature failure at the socket [26]. Hence, the inherent properties differences of the steel and GFRP reinforcements' behaviour resulted in significant differences in the behaviour of socket connection.

Replacing GFRP with steel will address corrosion issue and help mitigating the durability problem of such structures. The GFRP bars have a higher strength-to-weight ratio compared to steel reinforcement, however, they have a lower modulus of elasticity. The stiffness of the structural elements due to the lower modulus of elasticity of GFRP can be enhanced by using a higher reinforcement ratio so that they can perform similar to steel-RC structures. This has been reflected in the well-stablished design standards on GFRP-RC, (e.g. ACI 440.11–22 [27]). It's also worth noting that the compression failure of concrete (compression-controlled) typically governs the design of GFRP-RC. Additionally, in the case of tension failure, due to the elastic behaviour of GFRP, it does not exhibit a ductile behavior similar to steel-RC.

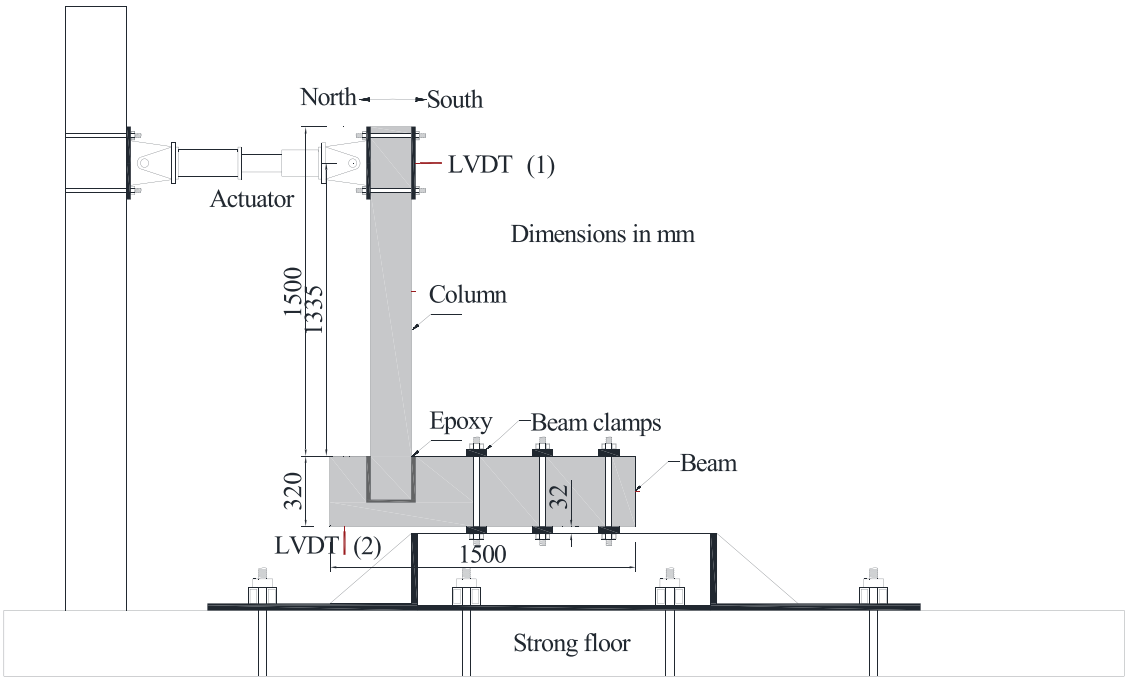

Fig. 2. Test setup for reference connections [26].

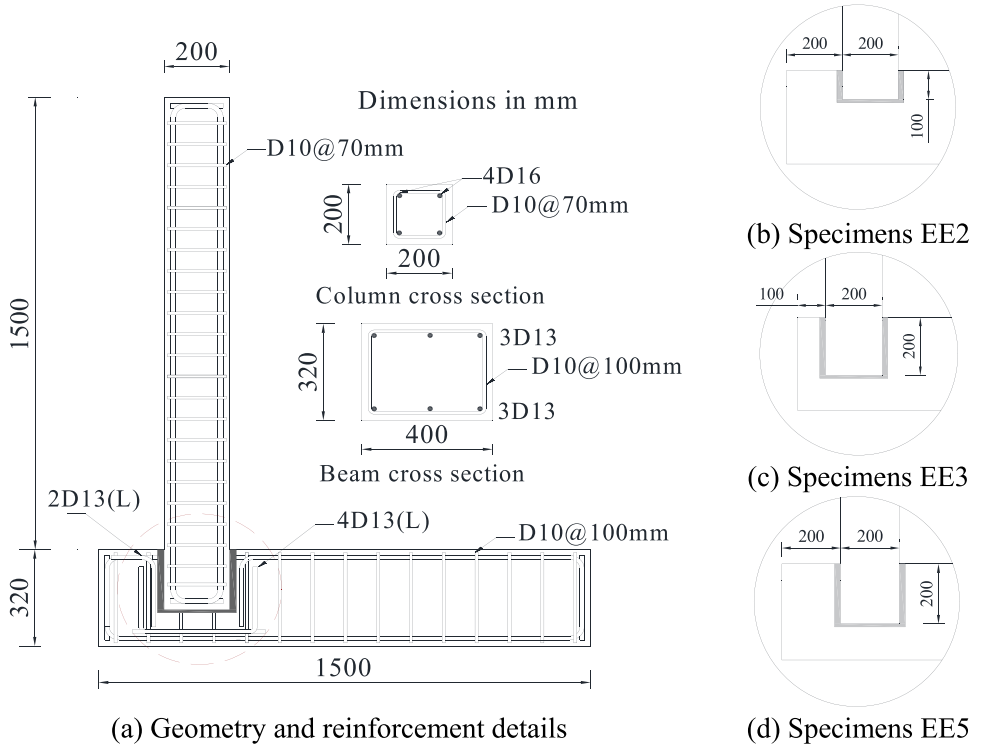

Fig. 3. Geometry and reinforcement details for refence specimens [26].

These significant differences limit the applicability of available design guidelines for socket connections in steel-reinforced structures to GFRP-reinforced structures. The lack of understanding the behaviour of socket connection in GFRP-reinforced concrete structures has limited their real-life applications. However, the combination of benefits from precast concrete and noncorrodible nature of GFRP enhance its suitability to be used in jetty structures where it is difficult to use cast-in-place concrete at these structures. To address these challenges, a numerical model for GFRP-RC precast socket connections was developed using nonlinear finite element modelling. The experimental results adopted from a previous study [26] were used to validate the accuracy of the numerical model. The validated model was then employed to examine the influence of socket depth, concrete depth under the socket, size of the beam, socket-filling material, and column reinforcement ratio on the behaviour of socket connections. The results were critically discussed, and design recommendations were provided to avoid local

Table 1
Properties of GFRP reinforcement.

Bar No.	Bar diameter (mm)	Cross section Area (mm^2)	Tensile Modulus of Elasticity (GPa)	Ultimate Tensile Strength f_{fu} (MPa)	Ultimate strain in tension (ε_{fu})
D 10	9.5	71	62.50	1315	0.023
D 13	12.7	129	61.30	1282	0.021
D 16	15.9	199	60.00	1237	0.021
D 19	19.1	284	60.50	1270	0.021
Bolt #20	20	314	53.0	890	0.017

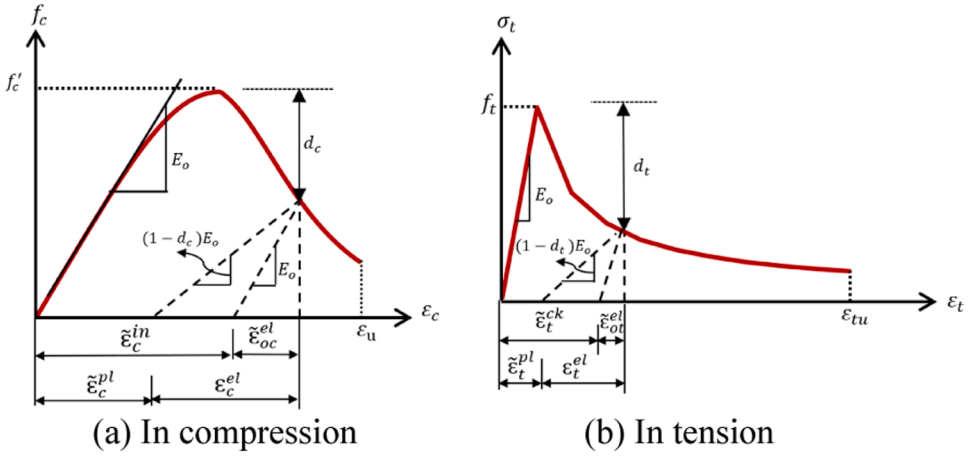

Fig. 4. Concrete material definition.

immature failure modes and provide a safe design for the GFRP-RC connections with sockets. The results of this study can be used to ensure proper design of GFRP-RC socket connections and optimize the performance of precast GFRP structures, which can facilitate their design and also help reduce construction time and maintenance costs.

2. Reference experimental tests for validation

A series of tests on precast GFRP-reinforced socket connections at the University of South Australia [26] were considered in this study for the model verification. The experimental test setup is shown in Fig. 2. As shown, the beam-column assembly was placed upside down on the strong floor and was specially designed in a way that the beam could rotate at the beam-column end, simulating the real-life scenario in frames of jetties. In these structures where GFRP is a perfect reinforcement alternative, the primary design forces come from the lateral loads while the axial load is considered minor. In addition, the presence of the axial load offers benefits in confining the connection. Therefore, to consider the most critical scenario, the lateral load was applied to the top of the column while no axial load was provided in the reference study [26]. The general dimensions and reinforcement arrangement of the beam and columns are shown in Fig. 3-a. The beam cross section was 400 mm × 320 mm and was reinforced by 3D13 top and bottom GFRP bars as well as ligatures of diameter 10 mm each at 100 mm spacing. The column cross-section was 200 mm × 200 mm and was longitudinally reinforced by 4D16 GFRP bars and transverse ligatures of diameter 10 mm spaced 70 mm apart. Both columns and beams were cast using high-strength concrete of strength 82.4 MPa. The properties of the GFRP reinforcement as supplied by the manufacturer are listed in Table 1.

In this test series, the column and beam were assembled by prefabricated sockets inside the beam. Epoxy resin was utilized to fill the 20 mm side gap between the beam and the column and the 10 mm from the bottom of the column. Epoxy was used instead of conventional grout due to its advantages including its non-shrinkage characteristics, high workability, high strength, and fast assembly. The compressive strength of epoxy was 93.5 MPa which was greater than the strength of the connected elements and had a modulus of elasticity of 2.3 GPa. Three specimens with different connection details, as shown in Fig. 3, were selected to be the basis for this numerical study to validate the accuracy and reliability of the developed numerical model under different conditions. The first specimen named EE2. In this specimen, the column embedded depth into the socket was equal to 100 mm and with an overhanging beam of 200 mm. The second specimen named EE3 had a 200 mm embedded depth into the socket and a 100 mm overhanging length. The last specimen named EE5 had an embedded depth of 200 mm and an overhanging length of 200 mm. An additional bolt of diameter 20 mm was provided in the connection of this specimen using a prefabricated duct of diameter 32 mm. The bolt had a length of 360 mm and was bonded using epoxy adhesive.

3. Numerical model

The nonlinear finite element software ABAQUS was employed to develop a numerical model for GFRP-reinforced precast socket connections. Details about the numerical model are discussed in the following sections.

3.1. Definition of concrete material

The behaviour of concrete material was simulated in the study using the concrete damage plasticity model, which is a continuum-based plasticity model [28]. This model considers two main modes of failure, which are tensile cracking and concrete crushing. This material model was extensively used in previous studies and demonstrated its efficiency to capture the nonlinear response of various types of cast in place and precast connections [29–32]. The employment of this model necessitates the definition of several parameters as discussed in the following sections.

- Uniaxial compressive behaviour: The behaviour of concrete under uniaxial compression is described by Thorenfeldt et al.'s model [33], which can be represented by Eq. (1). This model can be used for a wide range of concrete grades from 15 MPa to 125 MPa.

Table 2
Plasticity parameters considered in the models.

Dilation angle	Eccentricity	*Kc*	σ_{b0}/σ_{c0}
36	0.1	0.667	1.16

$$\frac{f_c}{f_c^{'}} = \frac{n\left[\frac{\varepsilon_c}{\varepsilon_o}\right]}{n-1+\left[\frac{\varepsilon_c}{\varepsilon_o}\right]^{nk}} \tag{1}$$

where, f_c is the compressive stress corresponding to strain ε_c, $f_c^{'}$ is the cylinder strength, ε_o is the strain corresponding to a stress equal to $f_c^{'}$, and the other parameters n and k are model's parameters which were taken equal to $n = 0.8 + \frac{f_c^{'}}{17.25}$ and $k = 0.67 + \frac{f_c^{'}}{62} \geq 1$ [34].

To define the compressive inelastic behaviour of concrete, the input data should be introduced in terms of an inelastic crushing strain $\tilde{\varepsilon}_c^{in}$ and the corresponding stress f_c according to Eq. (2) and Fig. 4-a.

$$\tilde{\varepsilon}_c^{in} = \varepsilon_c - \tilde{\varepsilon}_{oc}^{el} = \varepsilon_c - \frac{f_c}{E_o} \tag{2}$$

where the initial modulus of elasticity E_o can be taken equal to $4700\sqrt{f_c^{'}}$ [35],

- Uniaxial tensile behaviour: The behaviour of concrete under uniaxial tension is defined using the model proposed by Aslani and Jowkarmeimandi [36]. According to this model, a linear relation is assumed between the stress and strain up to the point where the concrete reaches its tensile strength, beyond which the behaviour of the concrete is described as,

$$\sigma_t = f_t\left[\frac{\varepsilon_{to}}{\varepsilon_t}\right]^{0.85} \tag{3}$$

where σ_t is the tensile stress corresponding to tensile strain ε_t, $\varepsilon_{to}$is the strain at the point of maximum tensile strength f_t which was taken equal to $0.33\sqrt{f_c^{'}}$ [37].

Similar to the definition of compressive behaviour, the concrete behaviour is introduced to the model in terms of cracking strain $\tilde{\epsilon}_t^{ck}$ and the corresponding stress σ_t according to Eq. (4) and Fig. 4-b.

$$\tilde{\varepsilon}_t^{ck} = \varepsilon_t - \tilde{\varepsilon}_{ot}^{el} = \varepsilon_t - \frac{\sigma_t}{E_o} \tag{4}$$

3.1.1. Damage parameters

Damage parameters for concrete $d_c = 1 - \frac{f_c}{f_c^{'}}$ and $d_t = 1 - \frac{\sigma_t}{f_t}$ [22] should be also introduced along with the behaviour in both compression and tension, respectively, as shown in Fig. 4. The damage parameters are included in the model in the strain softening region of the introduced stress-strain relationship. These parameters are used to automatically convert the inelastic compressive strains $\tilde{\varepsilon}_c^{in}$ and cracking strain $\tilde{\varepsilon}_t^{ck}$ into plastic compressive strains $\tilde{\varepsilon}_c^{pl}$ and plastic tensile strain $\tilde{\varepsilon}_t^{pl}$, respectively, according to Eq. (5) and Eq. (6).

$$\tilde{\varepsilon}_c^{pl} = \tilde{\varepsilon}_c^{in} - \frac{d_c}{(1-d_c)}\frac{f_c}{E_0} \tag{5}$$

$$\tilde{\varepsilon}_t^{pl} = \tilde{\varepsilon}_t^{ck} - \frac{d_t}{(1-d_t)}\frac{\sigma_t}{E_0} \tag{6}$$

3.1.2. Plasticity parameters

Certain plasticity parameters should be introduced to reflect the behaviour of the concrete in the CDP material model. These parameters include dilation angle, eccentricity, coefficient *Kc*, the ratio of concrete biaxial compressive strength to uniaxial compressive strength (σ_{b0}/σ_{c0}), and viscosity parameter μ. The recommended dilation angle for concrete is 31 to 42 [37], with 36 being the most appropriate value [29]. The eccentricity is commonly taken as 0.1 [28] indicating a consistent dilation angle across different levels of confining pressure. The value for the ratio (σ_{b0}/σ_{c0}) is a concrete material parameter which can be calculated using laboratory tests. Alternately, a value of 1.16 has been widely adopted [28,38]. The coefficient *Kc* represents the ratio between the second stress invariant on the tensile meridian and the compressive meridian which should be between 0.5 and 1 at first yield. Table 2 lists the used values of the plasticity parameters. In this study, the dilation angle, eccentricity value, σ_{b0}/σ_{c0} ratio, and *Kc* coefficient were taken as 36, 0.1, 0.667, and 1.16, respectively [29,32]. The viscosity parameter μ is utilized to address convergence issues in strain-softening material models, where a small value is preferred to mitigate non-convergence problems and minimize mesh size effects. However, it is crucial to control the viscosity parameter appropriately to avoid excessively stiff solutions. Therefore, a sensitivity analysis was conducted to determine the appropriate value for the viscosity parameter, which will be discussed in a subsequent section.

3.2. Epoxy resin

Samples of epoxy resin were tested during the main experimental program, and an average axial compressive strength of 93.5 MPa and modulus of elasticity of 2.3 GPa were reported. The experimental results for the stress strain curve for the epoxy as reported in [26] were considered to accurately define the behaviour of epoxy resin. The tensile strength of epoxy was taken according to the manufacturer's data. CDP model was also used to define the behaviour of epoxy resin as recommended by [39].

3.3. GFRP reinforcement

GFRP reinforcement behaves as linear elastic material up to the failure. Therefore, the properties of both longitudinal and transverse reinforcement were defined as elastic material up to the failure. The maximum strength, modulus of elasticity, and Poisson's ratio for GFRP depend on the bar diameter. These properties were taken according to the test data presented in Table 1.

3.4. Elements

The concrete beam, column, and epoxy volume inside the socket were modelled using the eight-node 3D element C3D8R. This element is a continuum with reduced integration and hourglass control option with three degrees of freedom at each cone. The GFRP reinforcement was modelled using the T3D2 truss element, which has two nodes and three degrees of freedom per node.

3.5. Interaction between parts

Several interactions between different parts of the model were considered to effectively simulate the reference specimens. The interaction between the epoxy resin and surrounding concrete was simulated using surface-to-surface contact. To define the properties of the surface contact, hard contact was employed in the normal direction and Penalty property was used to define the contact in the tangential direction using friction coefficient to account for slippage between the two surfaces. Because the coefficient of friction between epoxy and concrete depends on the surface condition, the chosen value was calibrated to determine the most appropriate value (This will be discussed in the following sections). While no slippage of GFRP bars was observed during the experimental test, the interaction between the reinforcement and concrete was defined using embedded interaction. However, using the

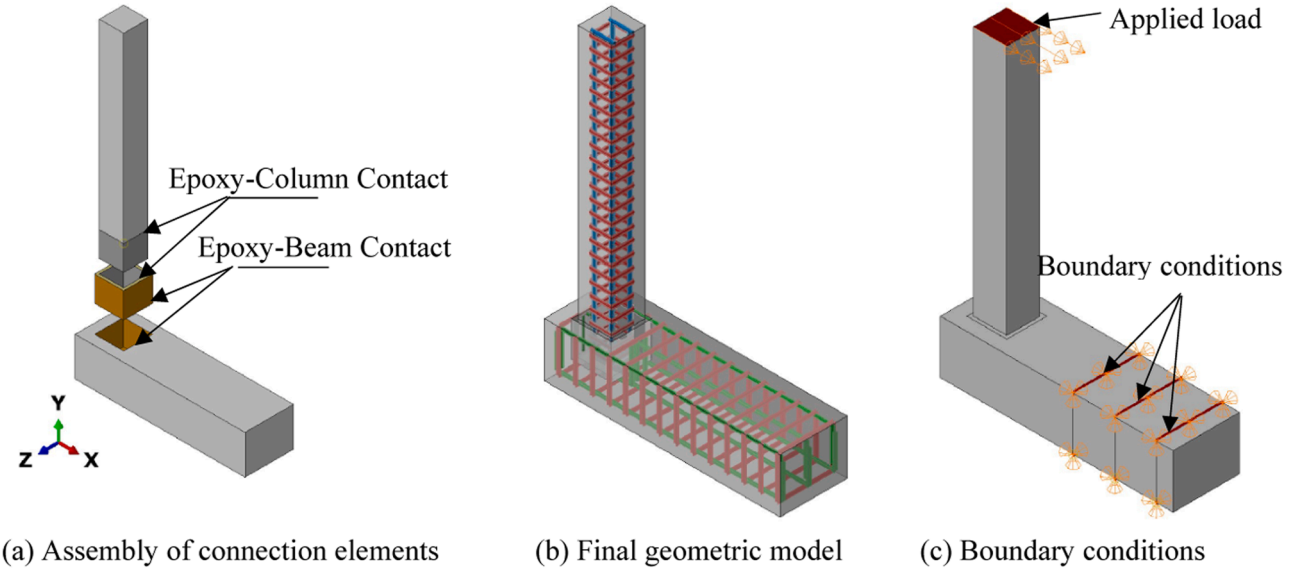

Fig. 5. Details of the developed numerical model.

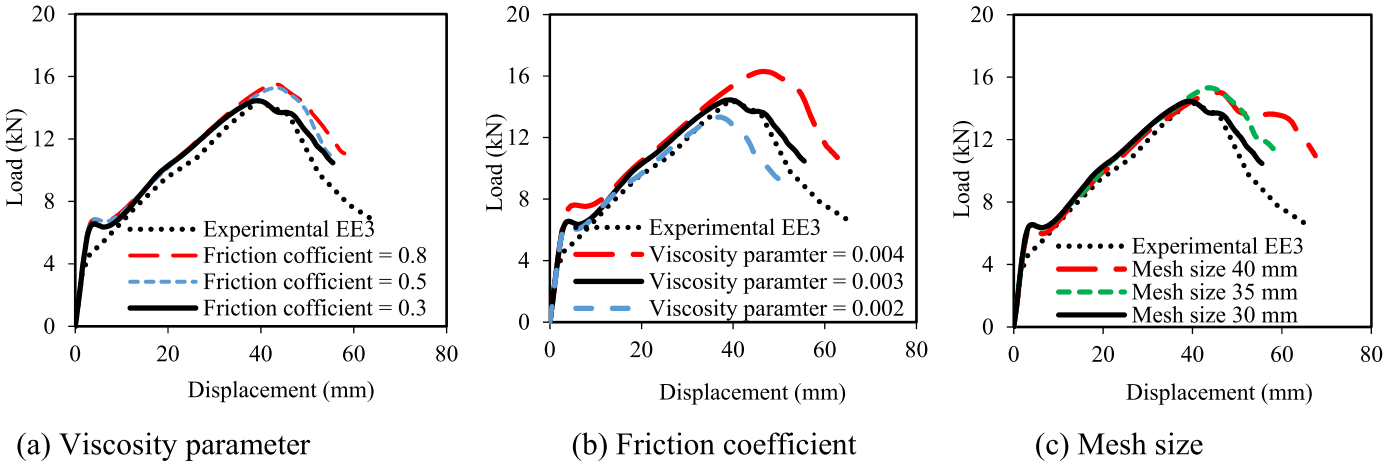

Fig. 6. Calibration of model parameters.

embedded interaction, the use of the CDP model offers a simple indirect way to account for the interaction between reinforcement and concrete such as bond slippage by considering the tension stiffening model which can be applied to simulate the transfer of load across cracks. This approach showed its efficiency in previous studies [29].

3.5.1. Simulation of test setup

Fig. 5 shows the geometric model for specimen EE3. Three 3D parts were created for the beam, column, and epoxy volume. For the assembly of the specimens, surface-to-surface contact was used between the inner surfaces of the epoxy and the outer surface of the column. The same interaction was used between the outer surface of the epoxy and the inner surfaces of the beam socket as shown in Fig. 5-a. The GFRP reinforcement was modelled as embedded reinforcement in the concrete. To simulate the support conditions of the experimental study, the boundary conditions were applied in the model at the location of the beam clamps by constraining the translation degree of freedom at these nodes. The lateral load was then applied at the top end of the column using a displacement control regime.

4. Verification of the accuracy of the numerical model

As mentioned, three specimens with different connection details were used to better verify the accuracy of the developed numerical against different parameters. The model of specimen EE3 was first developed and used to perform sensitivity analysis for choosing the appropriate values of the viscosity parameter, friction coefficient, and mesh size. After determining the most suitable values for these parameters, the two other specimens were examined to confirm the capability of the numerical model to detect the behaviour of GFRP-RC precast socket connections under different conditions.

4.1. Selection of the friction coefficient value

The value of the coefficient of friction plays a significant role in defining the actual contact behaviour between epoxy and concrete. In the experimental tests, the specimen's failure occurred mainly at the socket location due to stress concentration and slippage between the two materials. The value of the coefficient of friction between the epoxy and concrete is a challenging parameter which is difficult to be measured during the reference experimental test. It was reported from previous experimental tests on the frictional behaviour of different types of epoxy

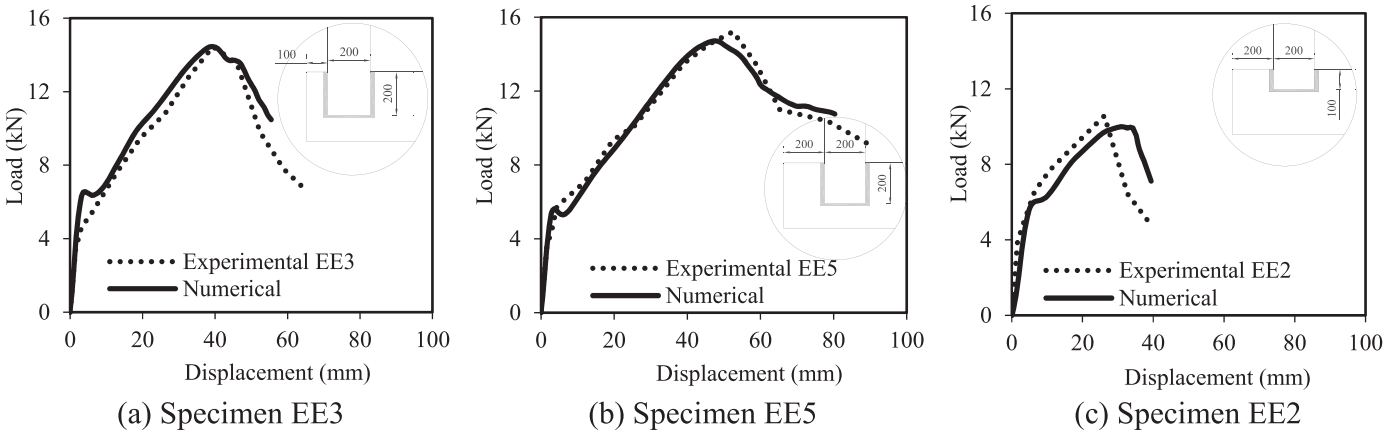

Fig. 7. Comparison between obtained load displacement curves and experimental ones.

that the coefficient of friction for epoxy ranged between 0.2 to 1.0 depending on the loading rate [40]. The use of a high coefficient of friction can improve the connection's integrity and reduce slippage, leading to an overestimated strength of the connection. Conversely, smaller values may result in underestimated capacity. In this study, three different values were examined (0.3, 0.5, and 0.8), and the load-displacement curves for each case were compared to the experimental data. Fig. 6-a confirms that as expected, increasing the coefficient of friction value led to an increase in the capacity of the connection due to controlled slippage and improved integrity of the connection. The results using coefficients of friction 0.8 and 0.5 gave an approximately similar capacity of 15.4 kN, while the test capacity was 14.5 kN. The obtained capacity is overestimated by approximately 6% compared to the experimental results. The most accurate solution was obtained using a coefficient of friction of 0.3, which gave a capacity of 14.45 kN, almost equal to the experimental result. This value for the coefficient of friction is in agreement with the recommendation from [41], where a value of 0.3 was found appropriate for the interaction between epoxy and concrete.

Both the finite element analysis and test results exhibited a similar trend, characterized by three distinct stages: pre-crack, post-crack, and post-peak. Before cracking, the initial stiffness was approximately the same in both sets of results. However, in the finite element model, the reduction of stiffness was observed at a relatively higher load, with a sharp drop in stiffness, while the test results exhibited a smoother change in stiffness. At the beginning of the analysis, where the load was low, the analysis was conducted within the linear elastic stage of concrete with specific loading increments to achieve convergence. Since boundary conditions and loads were assumed to be applied to nodes, which is a little different from experimental test conditions, and due to the perfect sharp re-entrant corners at the socket region, an increased risk of artificial stress concentration was expected. This risk stemmed from the theoretically infinite stress as well as infinite change in stiffness. The load increment was automatically reduced with several small increments until finding a convergence solution. Since a fine mesh was used, the solution was converged with a finite magnitude of stress. Subsequently, the material began to undergo nonlinear behaviour where stresses are controlled by plastic strains. These reasons led to obtaining a sharp transection point in the numerical solution that was not observed in the test results.

The discrepancy between the two sets of results can be also attributed to the idealized material constitutive model used to define both concrete and reinforcement, as well as the perfect interaction between model components, assuming all contact surfaces were perfectly connected. Additionally, the possibility of forming initial cracks, especially shrinkage cracks in concrete during the experimental test could lead to early micro cracking which was not simulated in the finite element models. Nevertheless, there was acceptable agreement between the pre-crack and post-peak behaviour in both sets of results.

4.1.1. Selection of viscosity parameter value

The viscosity parameter plays a critical role in the CDP model, especially for strain-softening material behaviour. It helps overcome non-convergence issues and mitigate mesh size effects. However, the value of this parameter needs to be carefully calibrated to ensure an accurate solution. If the value of this parameter is relatively large, it may lead to overestimated capacity and stiffer non-realistic behaviour and crack patterns. Previous research [29,37] has shown that using a smaller value can resolve convergence issues and the mesh size effect, but the value cannot be specified as it should be related to the size of the loading step. In this study, three different values (0.002, 0.003, and 0.004) were examined while keeping all other parameters constant, including a mesh size of 30 mm and a coefficient of friction of 0.3. The results presented in Fig. 6-b confirm the critical impact of the viscosity parameter. The initial stiffness for the three cases was almost the same. The lowest examined value of 0.002 resulted in the most accurate stiffness after cracking but the obtained capacity was 13.3 kN which was underestimated by 8% compared to the experimental results. The results using a viscosity parameter equal to 0.004 was found non-realistic where the capacity was around 16.3 kN (overestimated by 13%). As shown in Fig. 6-b, a value of 0.003 provides a reasonable result in terms of initial stiffness, ultimate capacity and post-peak degradation and hence is adopted here for further investigation.

4.1.2. Selection of appropriate mesh size

The CDP model is known for its dependence on mesh size. However, previous research suggests that viscoplastic regulations can resolve this issue for materials with strain-softening behaviour [29,37]. In this study, three mesh sizes were considered 30 mm, 35 mm, and 40 mm. Despite the use of viscoplastic regulations, the solution remained mesh size dependent, particularly in terms of post-peak behaviour, as shown in Fig. 6-c. However, this approach did address the problem of obtaining higher stiffness in numerical results, with the initial and post-crack stiffness being roughly the same across the three mesh sizes. The 35 mm and 40 mm mesh sizes were insufficient for detecting post-peak behaviour and crack propagation towards failure. The obtained capacities using mesh sizes of 35 mm and 40 mm were 15.3 kN and 15.1 kN, respectively. These capacities exceeded the experimental capacity of 14.5 kN by 5.5% and 4%, respectively. The most accurate results in terms of maximum capacity and post-peak behaviour were achieved using a mesh size of 30 mm. The capacity obtained in this case was 14.45 kN, which is nearly identical to the experimental test. However, while the three mesh sizes produced acceptable variations between numerical and test results in terms of maximum capacity, mesh size had

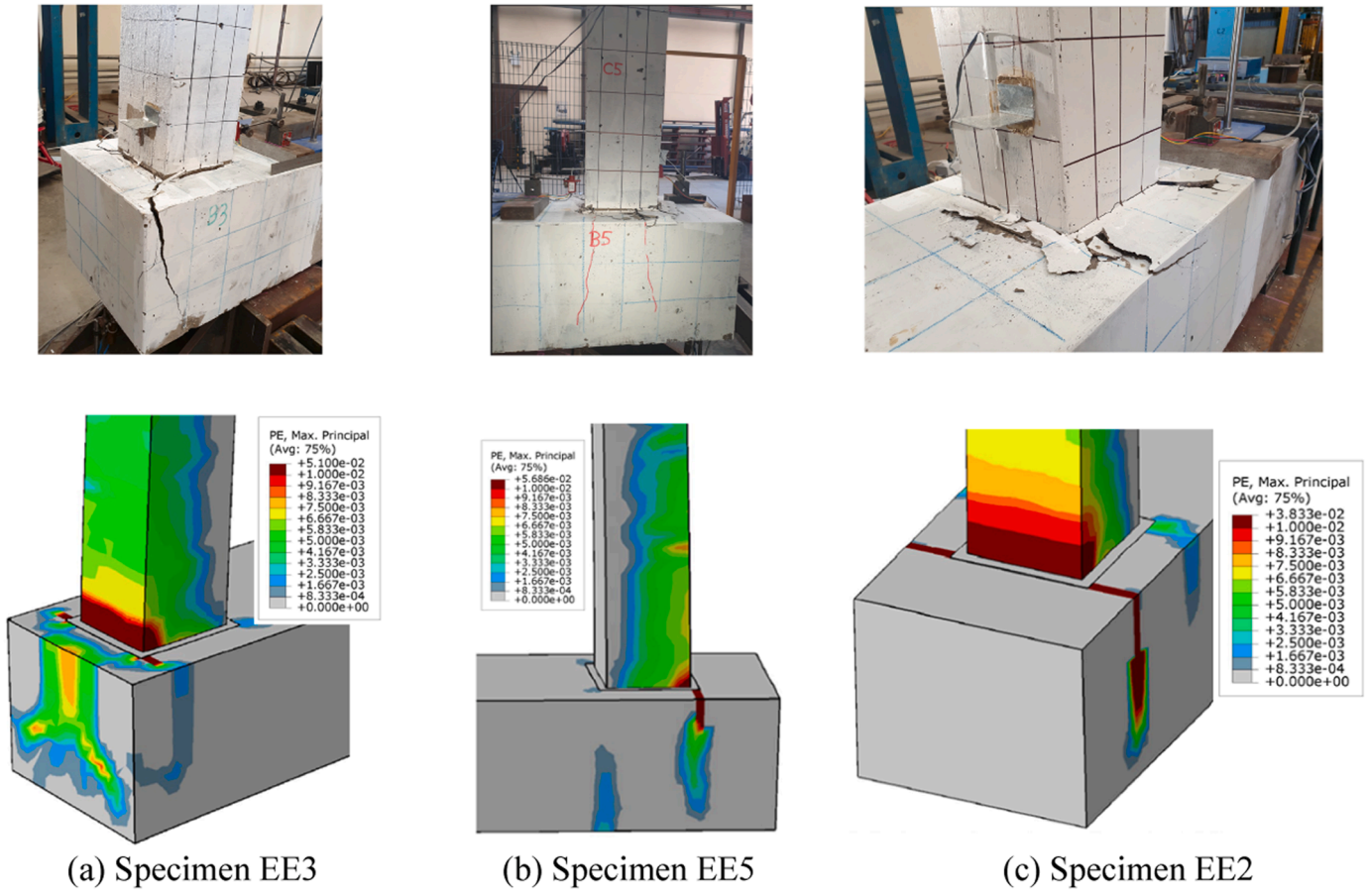

Fig. 8. Comparison between obtained crack patterns and experimental ones.

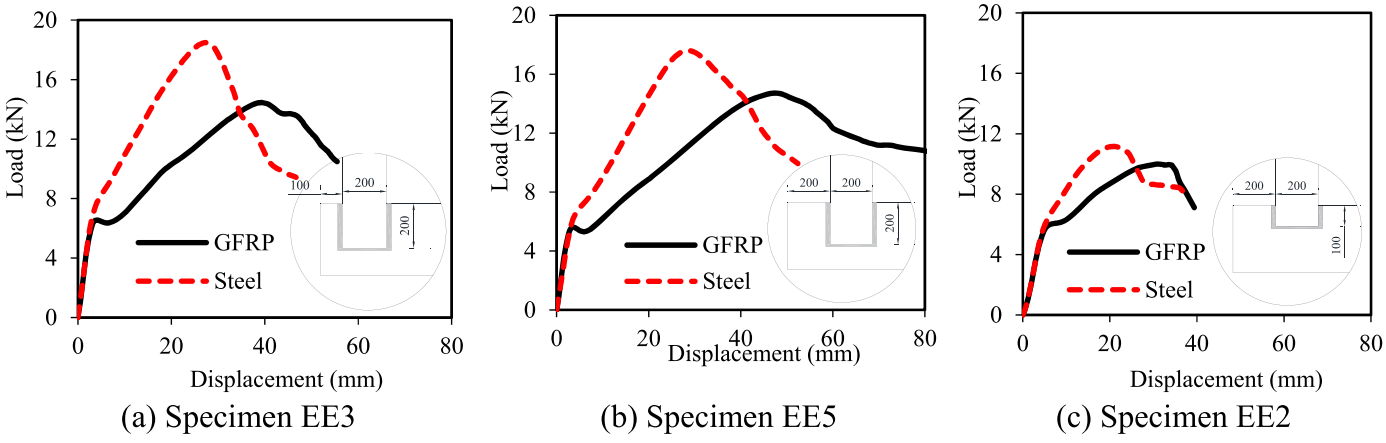

Fig. 9. Comparison between the behaviour of connections with GFRP and steel reinforced elements.

a significant impact on post-peak behaviour. Consequently, based on these findings, a mesh size of 30 mm is adopted for further investigation.

4.1.3. Model verification

The accuracy of a developed numerical model for different connections was validated by comparing the load-displacement behaviour and crack patterns of models for specimens EE3, EE5, and EE2 to the experimental results. The numerical model details were kept the same, except for the connections' geometry and details. The coefficient of friction, viscosity parameter, and mesh size were set to 0.3, 0.003, and 30 mm, respectively, based on calibration. The load-displacement behaviour of the specimens is shown in Fig. 7. The obtained peak load for specimens EE3, EE5, and EE2 were 14.45 kN, 14.8 kN, and 10 kN, respectively, while the maximum capacities from the experimental test were 14.5 kN, 15.2 kN, and 10.6 kN, respectively. As shown in Fig. 7, the results of the numerical model were in good agreement with the test results, except for some discrepancies in the post-peak behaviour of specimen EE2, which could be attributed to material deficiencies during the test that affected the actual friction coefficient while perfect and typical properties were assumed in the numerical models.

Moreover, the obtained crack patterns from the numerical modelling are in good agreement with the experimental crack pattern, as shown in

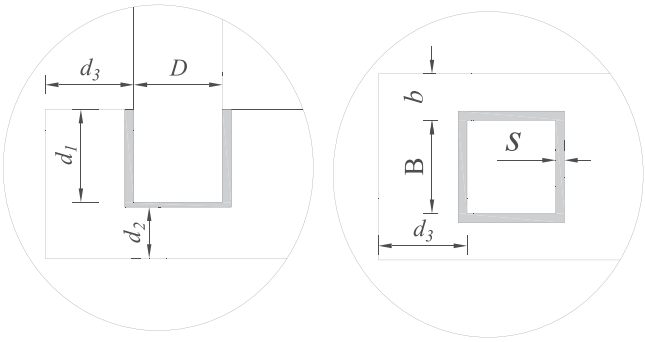

Fig. 10. Investigated parameters.

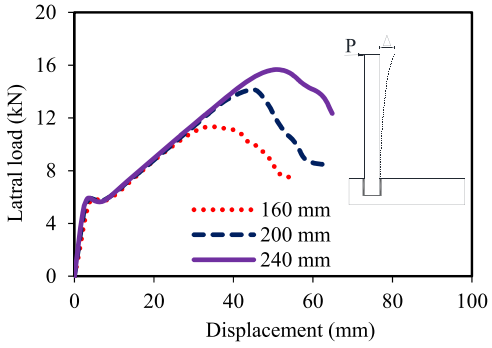

Fig. 11. Load displacement curves for connections with different socket depths.

Fig. 8. Specimen EE3 failed due to the formation of column cracks at the top surface of the beam and major beam cracks at the overhanging part. Specimen EE5 exhibited a similar crack pattern to the experimental ones where the connection failed due to column cracks and two beam cracks around the socket corners due to stress concentration. Specimen EE2 with shallow socket depth failed due to the formation of cracks at the top corners of the socket, similar to the experimental failure mode. These results reflect an acceptable accuracy of the developed numerical model for simulating the complex behaviour of GFRP-RC precast socket connection.

5. Behaviour of reference specimens with steel reinforcement

GFRP reinforcement in the calibrated specimens was replaced by conventional steel reinforcement of yield stress equal to 500 MPa in order to compare the behaviour of socket connections in the two cases. The elastic plastic model was used to define the behaviour of steel reinforcement with a modulus of elasticity equal to 200 GPa. The load displacement response was obtained for the three GFRP-RC specimens and their identical steel counterparts. The force-displacement responses are shown in Fig. 9 which indicates that the steel reinforcement resulted in a different response in terms of deformations, capacity, and deformation corresponding to maximum capacity. The difference in the behaviour is attributed to the linear elastic characteristics of GFRP reinforcement and its lower modulus of elasticity. This results in less confinement and more moving mechanism in the joint region. Such differences are expected between GFRP-RC elements and steel-RC elements having the same reinforcement ratio. This is accounted for in design guidelines and standards for GFRP-RC elements where the elements are designed with higher capacity reduction factors [27]. The initial stiffness of both reinforcement options was roughly equivalent.

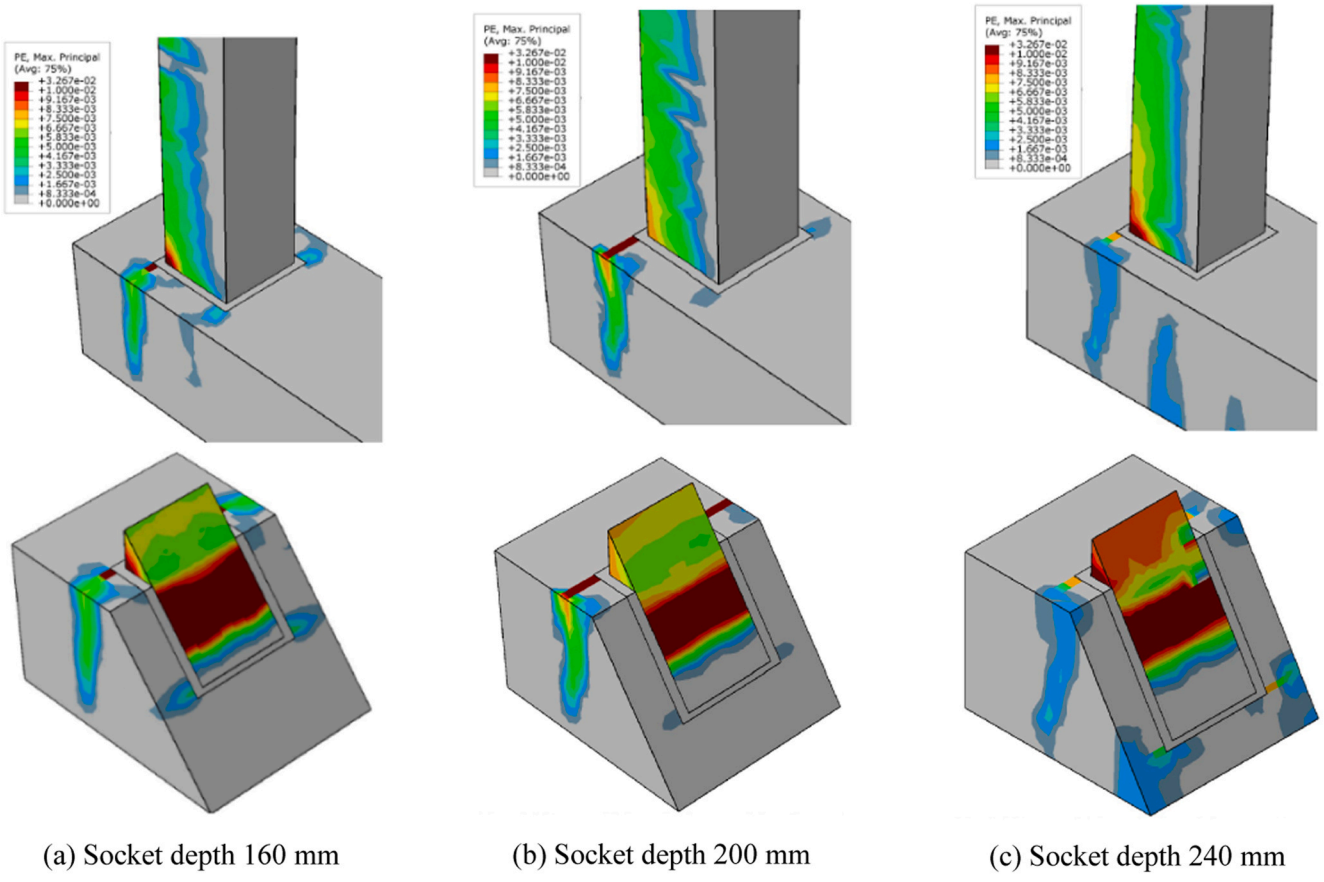

Fig. 12. failure mode for connections with different socket depths.

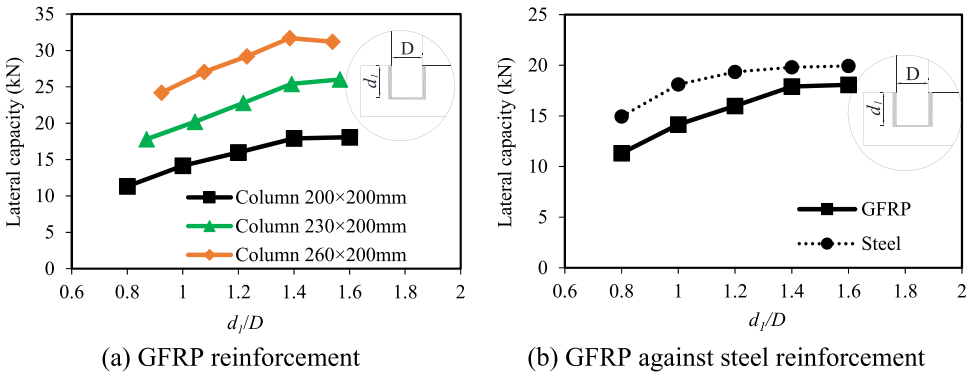

Fig. 13. Influence of different socket depths on the connection capacity.

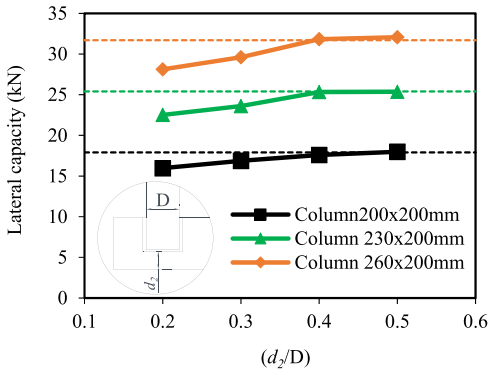

Fig. 14. Influence of the depth under the socket.

However, as they reached the cracking point, the stiffness of GFRP-RC specimens decreased more rapidly compared to the steel-RC specimens. Additionally, GFRP-RC exhibited more deformations than steel-RC due to the lower modulus of elasticity of GFRP reinforcement, impacting the serviceability and ductility of these structures. These fundamental differences ultimately resulted in the lower capacity of GFRP-reinforced connections when compared to their steel-reinforced counterparts. While there is no interface reinforcement between the beam and column in the socket region, the lateral capacity was improved by 27%, 20%, and 12% for specimens EE3, EE5, and EE2, respectively by replacing GFRP with steel. Due to such differences in the performance, the design recommendations for steel reinforced socket connections cannot be simply adopted for GFRP reinforcement. Subsequently, this excoriates the need for different column embedded depth into the beam to enhance the structural performance of GFRP-reinforced

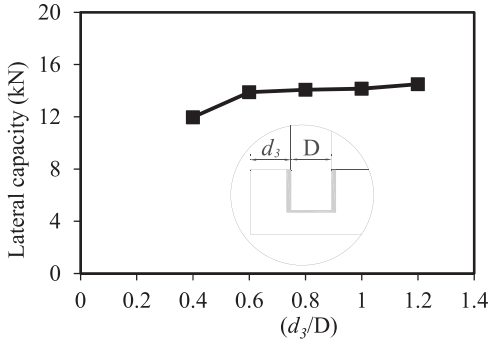

Fig. 16. Influence of different beam overhanging on the connection capacity.

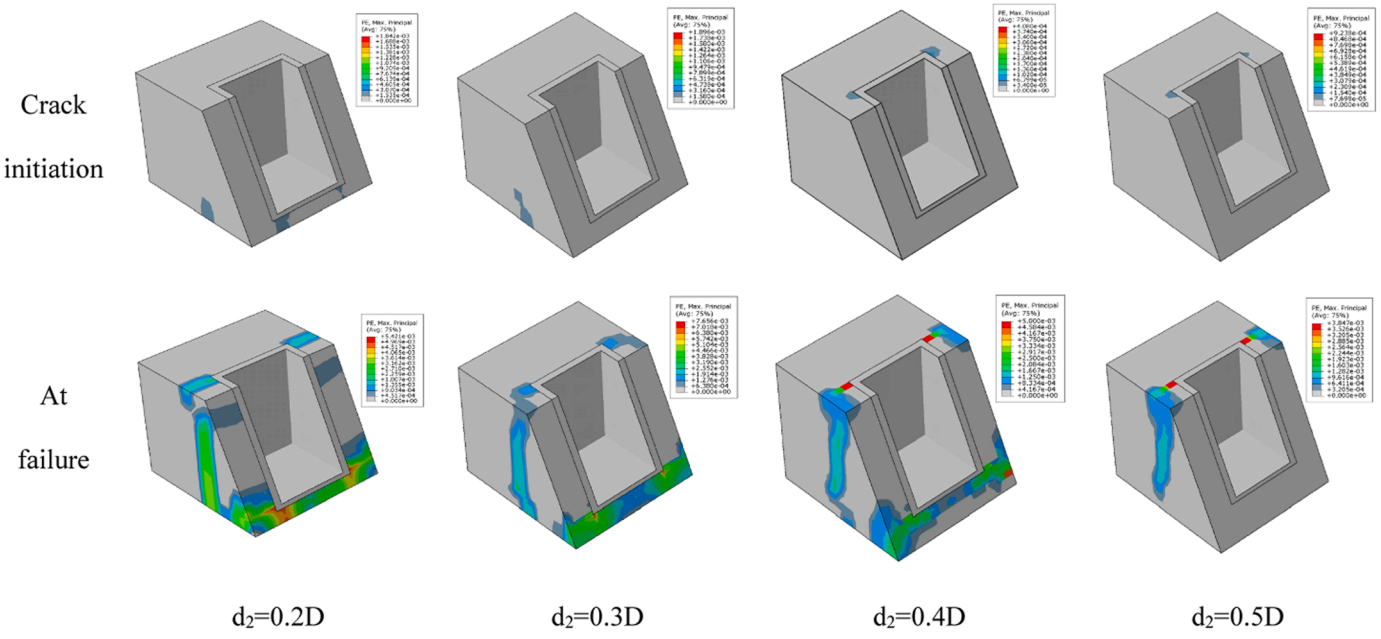

Fig. 15. Crack patterns for connections with different depths under the socket.

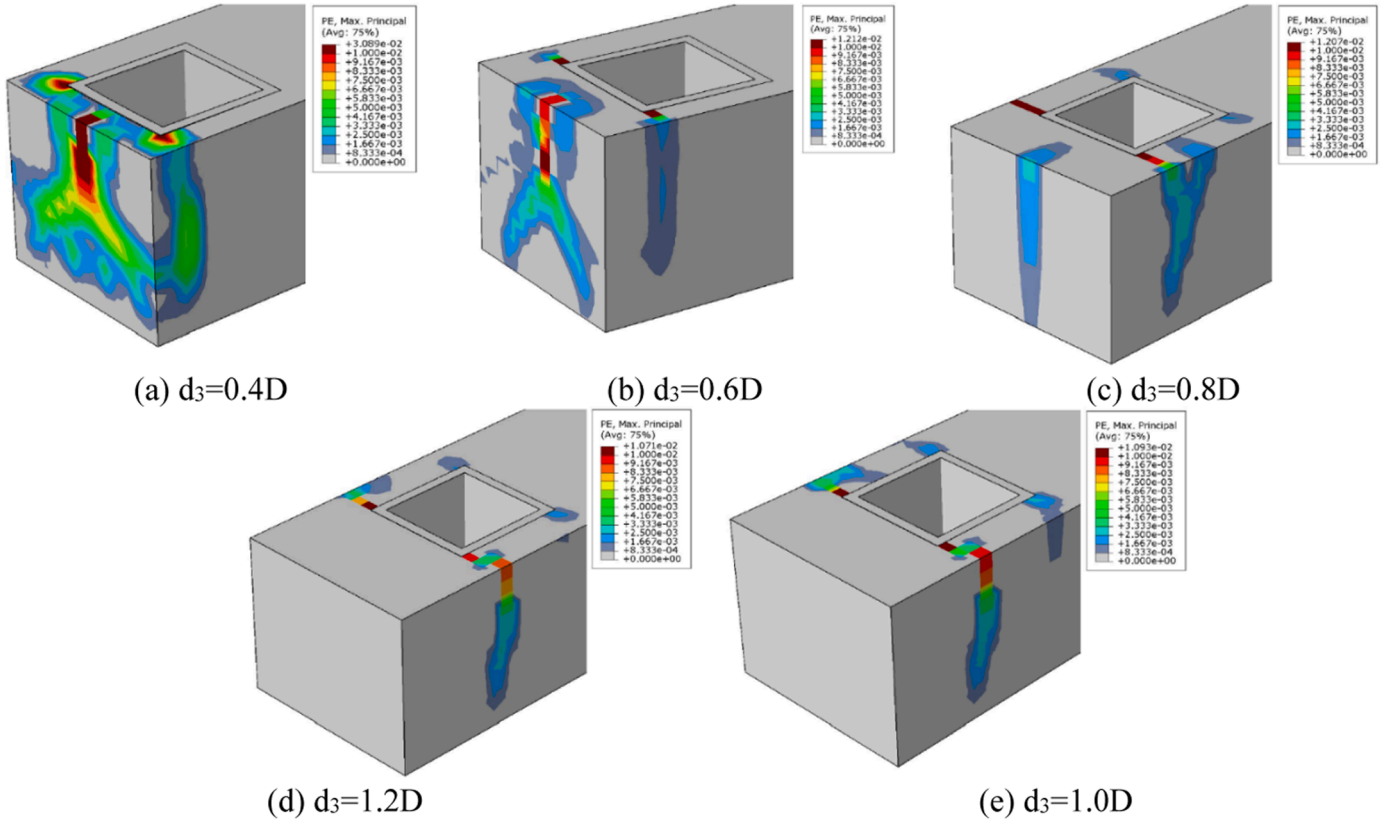

Fig. 17. Crack patterns for connections with different beam overhanging length.

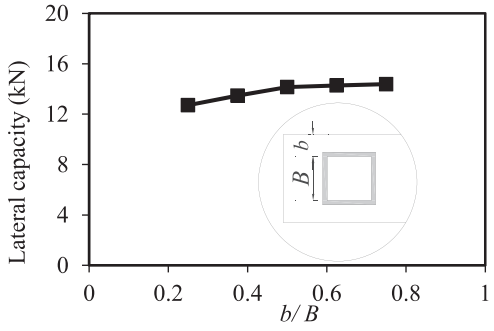

Fig. 18. Influence of different beam widths on the connection capacity.

connections in terms of having a stiffer connection with reduced deformations and higher capacity. To address this, an extensive parametric study was conducted to understand the critical parameters affecting the response of socket connection in GFRP reinforced precast concrete elements.

6. Parametric study

The calibrated numerical model was employed to investigate the influence of several parameters affecting the precast connections. The purpose of the parametric study was to understand the behaviour of GFRP-RC precast connections with socket and develop design recommendations to help to avoid some of the common immature failure modes observed previously during the experimental test [26]. The model with the same dimensions as specimen EE5 without any connection reinforcement at the connection region was considered as a reference. The column embedded depth in the reference specimens was 200 mm which was equal to the column thickness. It should be noted that the term column thickness in this study refers to the dimension of the column in the loading direction. The variables in the parametric study include column embedded depth d_1, depth under the socket d_2, overhanging length d_3, and overhanged beam width b (see Fig. 10).

6.1. Column embedded depth

Column-embedded depth is a critical parameter that governs the performance of the socket connection. A minimum embedded depth is necessary to ensure that the connection can transfer forces and moments effectively and develop its full capacity. It was found in the reference experimental test that an embedded depth equal to 0.5 of the column thickness was inappropriate and significantly reduced the connection capacity [26]. Also, a premature failure at the socket was observed with the embedded depth equal to the column thickness [26]. In contrast, previous studies on steel reinforced socket connections reported that a column embedded depth of more than 1.2 of the column thickness is sufficient to attain the connection capacity [5,11–13]. However, the required embedment depth has not been studied in the previous studies, and it is essential to examine the behaviour of GFRP-RC socket connections to get insights into the difference in the behaviour compared to that of steel reinforced ones. In this study, the behaviour of GFRP-reinforced socket connections with embedded depths of 160 mm, 200 mm, and 240 mm, corresponding to 0.8, 1.0, and 1.2 of the column thickness, respectively, were examined and compared. The maximum examined value was limited to 1.2 of the column thickness due to beam depth limitation. Load displacement curves, crack patterns, and peak strength were obtained to evaluate the effect of each embedded depth on the connection performance.

The load-displacement behaviour for connections with different socket depths is shown in Fig. 11. It can be noticed that the initial and post-crack stiffness remain consistent across the different embedded depths. However, the peak strength and deformation capacity are

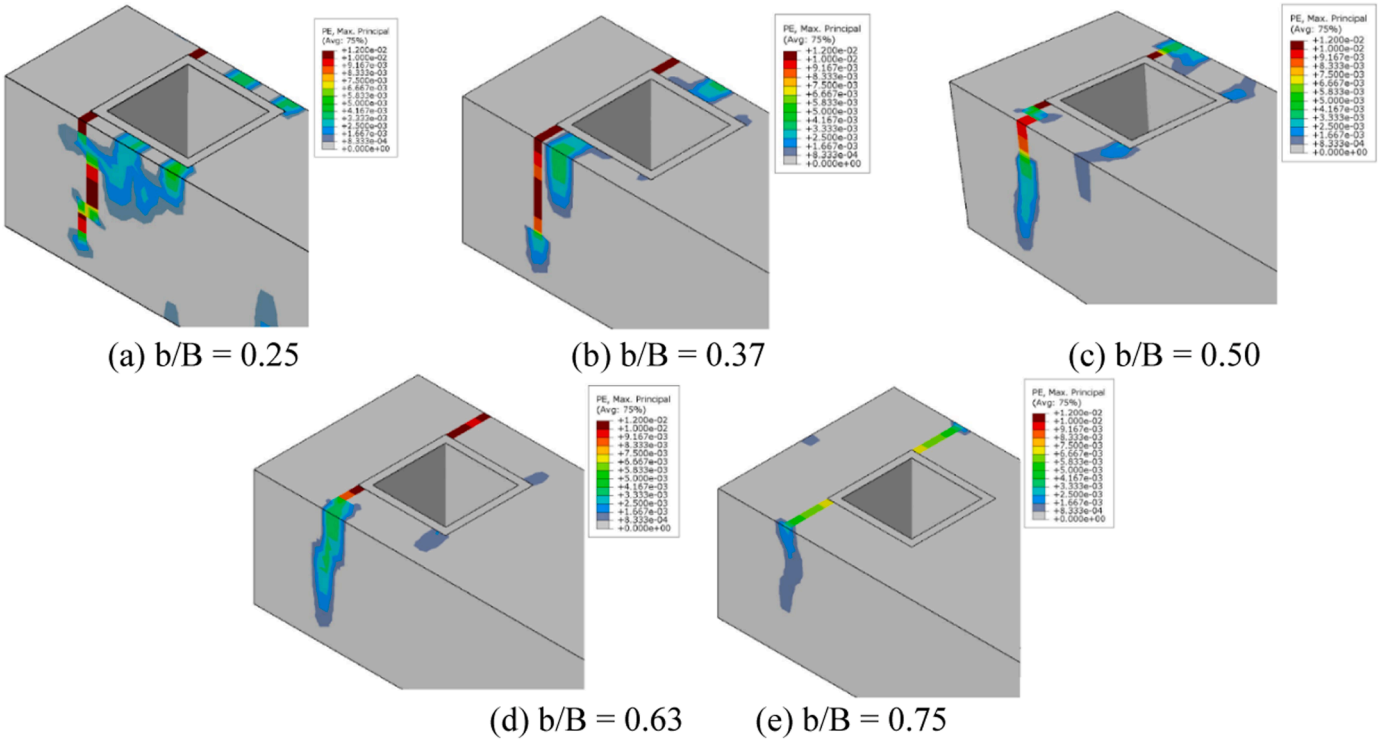

Fig. 19. Crack patterns for connections with different beam widths.

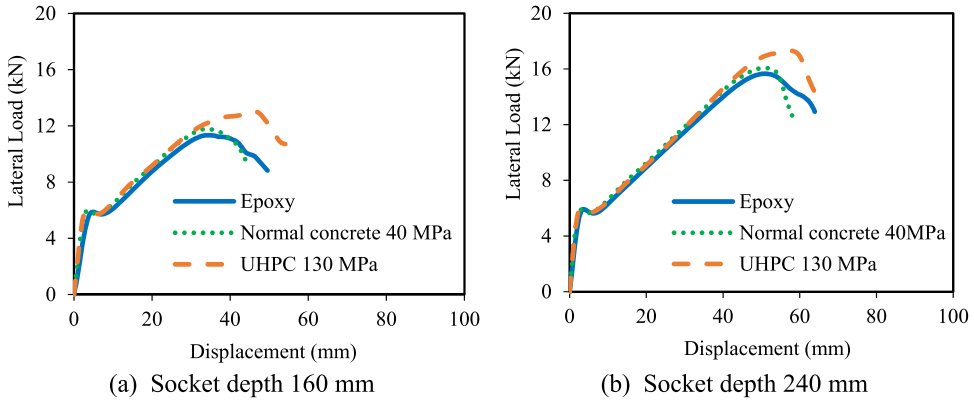

Fig. 20. Load displacement curves for different socket materials.

significantly influenced by the socket depth. The connection capacity was found to be 11.3 kN, 14.2 kN, and 15.7 kN for embedded depths of 160 mm, 200 mm, and 240 mm, respectively. The results reveal that increasing the embedded depth from 160 mm to 200 mm led to a 25% improvement in the capacity. Similarly, increasing the socket depth from 200 mm to 240 mm resulted in an 11% increase in capacity.

The strain of the tensile reinforcement of the column at the peak load was found equal to 0.0042, 0.0054, and 0.0063 for embedded depths of 160 mm, 200 mm, and 240 mm, respectively. The strain in GFRP reinforcement increased by 28% and by 17% up on increasing the embedded depth from 160 mm to 200 mm and from 200 mm to 240 mm, respectively. Moreover, as the lateral load increases, the column's rotation also increases due to the upward movement of the column's bottom end on the tensile side and the downward movement on the compression side. The upward and downward movement of the column was 2.7 mm and 2.4 mm for the embedded depth of 160 mm, respectively while the upward movement was limited to 1.1 mm and 0.88 mm and the downward movement was limited to 1.2 mm and 0.94 mm, for the embedded depth of 200 mm and 240 mm, respectively. These results indicate that this improvement is attributed to the effective transfer of forces through friction by increasing the contact area. Increasing socket depth offers better integrity of the structure and efficient load transfer within the connection.

The crack pattern for each case is shown in Fig. 12. All connections exhibited column flexural cracks at the end of the column. Specimen with a socket depth equal to (0.8D) failed due to the formation of cracks at the beam due to stress concentration around the socket as shown in Fig. 12-a. The visualization of cracks through the saw cut plan passing through the socket and the column indicates that the column suffered severe damage at the socket region indicating a premature failure at the socket. These cracks were approximately at the column base. Also, some cracks were propagated at the bottom of the socket due to stress concentration at the corners of the socket. The crack pattern for connection with a socket depth equal to (1.0D) was approximately similar to that with a socket of a depth of 160 mm. However, due to the increased socket depth, the developed cracks around the socket were reduced due

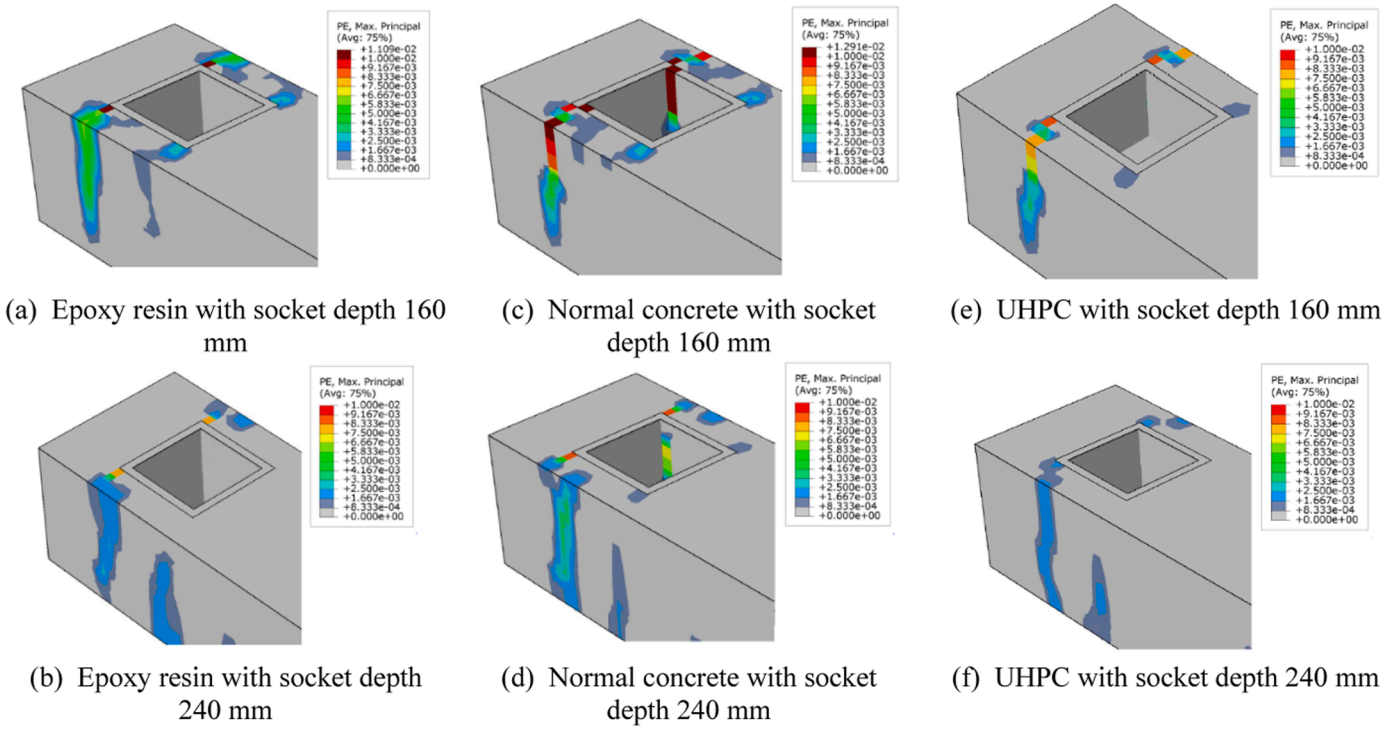

Fig. 21. Crack patterns for connections with different socket materials.

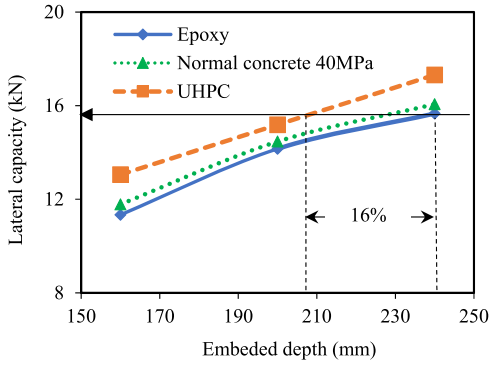

Fig. 22. Influence of socket material on the capacity of connection with different socket depths.

to the improved load transferring mechanism with increasing socket depth. Increasing the socket depth to 240 mm (=1.2D) reduced the stress concentration around the top of the socket and limited the left side crack. However, a new crack started to propagate from the bottom toward the top of the beam due to the increased stress concentration around the corners of the socket bottom. These cracks are attributed to the reduced volume of concrete underneath the socket.

The results confirm the significant impact of the socket depth on the capacity and failure mode of the socket connections. It seems none of the above connections could fully transfer the applied load due to the immature failure of the connections. The socket depth should be optimized to ensure sufficient socket depth while avoiding the formation of cracks at the bottom corners of the socket. To investigate this object, the beam depth was increased to 460 mm to allow for examining a wide range of socket depths. Three different column thicknesses, D, were hence considered, 200 mm, 230 mm, and 260 mm. The column width was kept constant in order to keep the beam width constant. Five different embedded depths were examined for each column thickness, and the peak strength was obtained. Moreover, an additional set of models with steel reinforcement was also considered to compare the results for the column thickness of 200 mm.

The results in Fig. 13-a confirm that increasing the socket depth significantly improves the connection capacity. However, the capacity remained relatively unchanged beyond a certain socket depth. The relationship between the normalized embedded depth to column thickness and the connection capacity is presented in Fig. 13-a. The results indicate that increasing the socket depth has a significant positive impact on the connection capacity for the examined column sections. Specifically, for a connection with a column thickness of 200 mm, a 75% increase in socket depth from 160 mm to 280 mm led to a remarkable 58% improvement in the connection capacity. Similarly, for a connection with a column thickness of 230 mm, increasing the socket depth by 60% from 200 mm to 320 mm resulted in a 43% increase in capacity. In the case of a connection with a column thickness of 260 mm, a 50% increase in socket depth from 240 mm to 360 mm led to a capacity improvement of 31%. A 10% increase in the socket depth resulted in an approximate capacity improvement of 7.8%, 7.1%, and 6.2% for the connections with column thicknesses equal to 200 mm, 230 mm, and 260 mm, respectively. These results suggest that optimizing the socket depth as a ratio of the column thickness can significantly enhance the connection capacity as long as the formation of cracks at the bottom corners of the socket is prevented.

The maximum capacity in the case of using steel reinforcement is compared with that obtained using GFRP reinforcement for a column of dimensions 200 mm × 200 mm (see Fig. 13-b). As shown, while the maximum capacity using GFRP reinforcement can be obtained with a socket depth of 1.4D, this was equal to 1.2D when steel reinforcement was used. However, the improvement of the capacity by increasing the socket depth from 1.0D to 1.2D was limited to 6%. These results are in good agreement with previous studies on steel reinforced socket connections where the full capacity was found to be achieved with a socket of depth of 1.0D to 1.2D [5,11–13].

Fig. 13 suggests that a minimum socket depth of 1.4D is needed to fully transfer the moment at the connection. Beyond this limit, the capacity of the connection remained relatively constant. This minimum required embedded depth was found greater than that required for steel

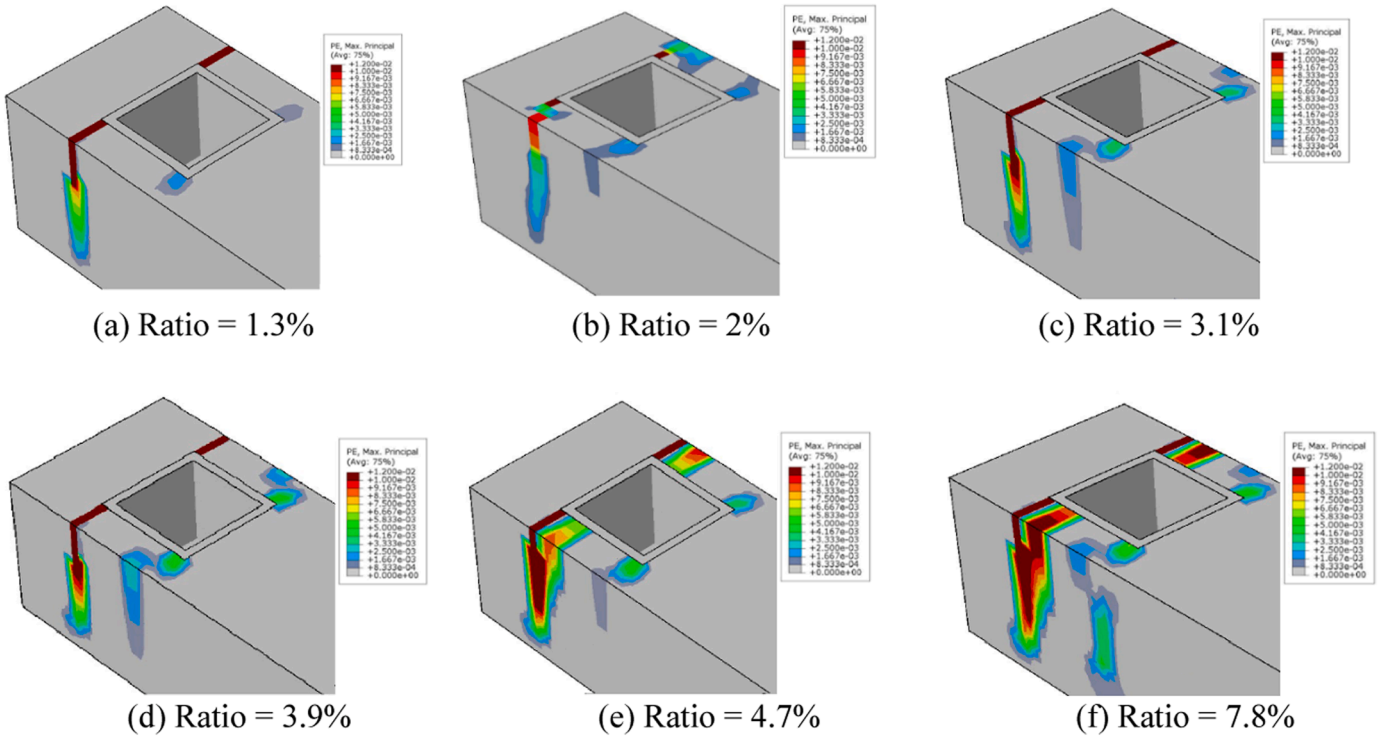

Fig. 23. Crack patterns for connections with different column longitudinal reinforcement ratio.

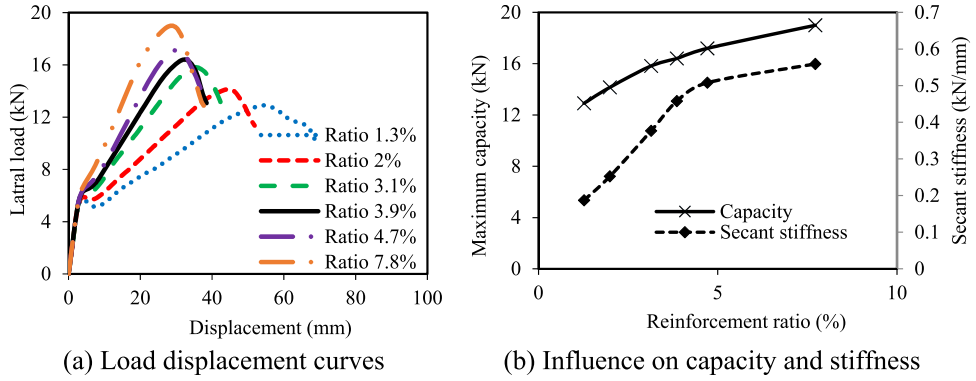

Fig. 24. Influence of column reinforcement ratio on the capacity of socket connection.

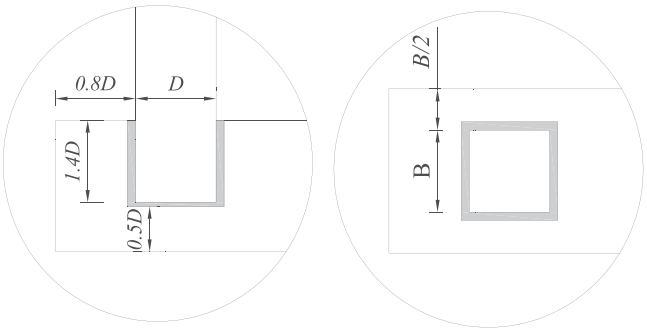

Fig. 25. Recommended details for GFRP socket connections.

reinforced socket connections. GFRP reinforced socket connection required greater embedded depth. The low modulus of elasticity for GFRP reinforcement affects the formation of cracks at earlier loads with relatively wider cracks. These cracks reduced the stiffness of the socket connection which resulted in a more flexible behaviour with larger deformations. This more flexible behaviour allows for some degree of movement which affects the area that the load is distributed on and increases the stress concentration due to localized deformations. This necessitates the use of greater socket depth to ensure a proper load transferring mechanism.

As shown in Fig. 13-a, in the case of a column thickness of 260 mm, increasing the socket depth beyond 1.4 times the column thickness resulted in a reduction in capacity. Investigating the stress pattern of this specimen, revealed that the failure was partially influenced by the stress concentration at the bottom corners of the socket. This was due to the reduced concrete depth under the socket. This observation emphasizes the importance of having sufficient concrete depth under the socket. To better understand this mechanism, additional series of models were generated in which the socket depth was set to 1.4D and the depth of concrete underneath the socket, d_2, was considered as a variable by changing the beam depth. The results for d_2 ranging from 0.2D to 0.5D are shown in Fig. 14. As shown in Fig. 14, the results indicate that increasing the depth of concrete underneath the socket gradually from

0.2D to 0.4D led to an improvement in the connection capacity, beyond which the capacity remained unchanged.

The crack initiation and failure mode of the connection depicted in Fig. 15 confirms that the depth underneath the socket has a significant impact on the connection's behaviour. For columns with dimensions of 200 × 200 mm, cracks began to propagate from the bottom of the beam and resulted in severe damage at failure under the socket when the depth underneath the socket, d_2 was equal to 0.2D or 0.3D. When d_2 increased to 0.4D or 0.5D while initial cracks were still initiated from the top surface of the beam (due to stress concentration around the socket corners) the stress concentration and damage beneath the socket were significantly improved. As shown in Fig. 15, the connection with d_2= 0.4D experienced a much lower level of damage under the socket, while in the connection with d_2= 0.5D, such damage was prevented. According to these results a minimum d_2 value of 0.5D is suggested to be considered in the design of GFRP-RC socket connections.

6.2. Beam overhanging length

The overhanging length, d_3 of the beam (from the edge of the column to the free end of the beam: see Fig. 10) is an important factor affecting the performance of the connection. In some situations, due to practical reasons, the columns are preferred to be located as close as possible to the edge of the beam. However, sufficient overhanging is needed to confine the socket and avoid immature failure. To investigate this, five overhanging lengths, ranging from 0.4D to 1.2D were considered while the beam width and socket depth were considered constant as in the reference model. The results, as shown in Fig. 16, demonstrate a drop in the capacity of the connection when the overhanging length is less than 0.6D. This is due to less effective confinement to the socket, resulting in significant cracks and damage at the overhanging side around the socket, as illustrated in Fig. 17. For the connection with an overhanging length of 0.6D or less, the crack initiation provides room for the column rotation inside the socket and hence results in a noticeable stiffness reduction. Subsequently, this results in stress concertation at the top level of the socket which led to the formation of cracks especially concentrated at the overhanging side, while no cracks developed around the socket corners on the other side (see Fig. 17). As shown in Fig. 17, the damage at the overhanging side can be limited by increasing the overhanging length of the beam to 0.8D or more overhanging length.

6.3. Beam width

Beam width is another parameter that can reflect the effect of side confinement to the socket. the size of the beam must be larger than the column to accommodate the socket, however significantly larger beam results in extra cost. The distance b on the side of the socket (see Fig. 10) should be large enough to accommodate the required reinforcement and prevent local failure of the socket in those regions. The effect of beam width on the socket connection was investigated considering five different beam widths: 300 mm, 350 mm, 400 mm, 450 mm, and 500 mm, corresponding to a beam oversize width to column width to (b/B) ratio of 0.25, 0.37, 0.5, 0.63, and 0.75, respectively. The beam overhanging length was kept constant as in the reference model and the only variation was the beam width. The results presented in Fig. 18 show that beyond a b/B ratio of 0.5 the capacity is not negatively affected. However, there was a 5% and 12% capacity drop when b/B was reduced to 0.37 and 0.25, respectively. This is due to the formation of significant cracks around the socket as shown in Fig. 19. According to these results, a minimum b/B of 0.5 should be considered for design. In other words, the width of the beam should be double that of the column.

6.4. Socket filling material

Socket material is responsible for achieving the proper integrity of the precast structure. While epoxy resin has various advantages such as high strength, fast assembly, high workability, and reduced curing time, it has a low modulus of elasticity. To evaluate and compare the performance of the connection with different filling materials, the use of ultra high performance concrete (UHPC), normal concrete of strength 40 MPa, and epoxy resin was evaluated. The material properties including stress strain relation, and modulus of elasticity for UHPC are different to those of traditional concrete. The constitutive material model for UHPC was adopted from [31]. The compressive strength of UHPC was 130 MPa and its tensile strength was 7.6 MPa [31]. The effect of socket filling material was examined for three socket depths of 160 mm, 200 mm, and 240 mm. The load displacement behaviour for the case of socket depth of 160 and 240 mm is presented in Fig. 20. Although normal concrete strength is approximately 45% of epoxy strength, the obtained load displacement curves for both materials were found almost similar. However, using normal strength concrete caused damage to the socket due to its reduced tensile strength compared to that of epoxy resin, as shown in Fig. 21. In contrast, the combination of high tensile strength and high modulus of elasticity for UHPC led to improved performance of the connection in terms of load displacement curve and failure mode. Therefore, the study suggests that UHPC can be a suitable alternative to epoxy resin in socket connections with the potential to enhance the structure's overall performance, as long as appropriate socket size is taken into consideration.

The maximum capacity with UHPC is improved by 16% compared to the corresponding connection with epoxy resin. Furthermore, Fig. 22 shows that the connection capacity which was achieved with an embedded depth of 240 mm using epoxy resin can be achieved by using UHPC with a reduced socket depth, resulting in a savings of about 16% of the socket depth. Although UHPC may require a longer curing time compared to epoxy resin, it can be a favourable solution to reduce the socket depth while maintaining the desired connection capacity. This reduction in socket depth can result in a reduction in beam depth and thus optimize the overall cost of the precast structure.

6.5. Column longitudinal reinforcement ratio, ρ_p

According to ACI 440.11–22 [27], the minimum and maximum longitudinal reinforcement ratio for GFRP in a column should not be less than 1% and more than 8%, respectively. In this study, for the reference connection, the longitudinal reinforcement ratio ρ_p was equal to 2%, in which a premature failure occurred due to stress concentration at the connection region. Decreasing the column reinforcement ratio can lead to more capacity reduction due to the failure of the column instead of the connection. While increasing its ratio increases the possibility of having a failure at the connection region. To examine the effect ρ_p, a range of ρ_p between 1.27% (provided by four GFRP bars of 12 mm diameter) to 7.8% (provided by eight GFRP bars of 22 mm diameter. All examined values resulted in the failure at the connection region (see Fig. 23). The load displacement behaviour of these models is shown in Fig. 24. The results show the significant impact of the longitudinal reinforcement ratio at the connection region on the obtained response. Increasing the column reinforcement ratio at the connection region significantly enhanced the stiffness which controls the lateral deformations and subsequently contributes to increased capacity. Increasing the column reinforcement ratio by 2.6% from (1.3% to 3.9%) resulted in an improvement in the connection capacity by 27%, while increasing the reinforcement ratio by 3.9% from (3.9% to 7.8%) improved the capacity by 15%. The additional reinforcement allowed the column to withstand higher loads without experiencing significant deformations. These results show that column reinforcement plays an essential role in the load transfer mechanism which accounts for the increase of the connection capacity with increasing the column reinforcement ratio. This increase in the column reinforcement ratio can only be locally applied at the socket region to improve its performance.

While the initial stiffness of all connections was almost the same (see

Fig. 24), the post-crack stiffness increased with an increase in the column reinforcement ratio. Additionally, the maximum capacity was obtained at an earlier displacement with an increase in the column reinforcement ratio. Fig. 24 also shows that the stiffness was significantly improved by increasing the column reinforcement ratio up to 3.9%. Increasing the reinforcement ratio beyond 3.9% showed a limited impact on the obtained stiffness. The increased stiffness of the column also resulted in a stiffer connection, which could transfer higher loads and moments between the beam and column. However, increasing the reinforcement ratio beyond 3.9% showed limited impact on the obtained stiffness, indicating that the optimal reinforcement ratio had been achieved. It is worth mentioning that a reinforcement ratio of 4% can be considered as the maximum practical ratio to ensure that the maximum reinforcement ratio does not exceed 8% at the lap splice location.

7. Practical outcomes

The results of this study provide simple practical considerations for the safe design of GFRP-RC precast connection and increase its application in harsh environment like jetty structures. The outcomes of this study are summarized in Fig. 25. which shows the recommended values for the safe design of GFRP-RC precast socket connections. A column embedded depth of 1.4D is recommended for achieving proper performance of the connection. The value is slightly larger than 1.2D which is commonly used for steel-reinforced socket connections [5,11–13]. The study also recommended that a sufficient depth of 0.5D should be provided under the socket. This value is also greater than that recommended for steel reinforced elements which is 0.25D [42]. The overhanging length is recommended to be not less than 0.8D and the beam width is recommended to be twice the column size. Although the current study showed that the last two parameters have a critical influence on the connection performance, no direct recommendations were previously mentioned for steel reinforced connections. Further studies should investigate the reinforcement detailing as well as the column cross-sectional shape and geometry on the behaviour of socket connections.

8. Conclusions

This study presents a numerical investigation on the behaviour of precast socket connections in GFRP-reinforced structures. Finite element models were developed and verified against large-scale experimental results, followed by a parametric study to investigate the influence of several key parameters affecting the socket connection behaviour including socket depth, concrete depth under the socket, size of the beam, socket-filling material and column reinforcement ratio. According to this study, the following conclusions can be drawn.

1. The utilization of socket connections in GFRP-reinforced structures is considered an efficient solution for accelerating the construction of jetties. However, achieving the required performance necessitates appropriate detailing of the connection.
2. Increasing the socket depth significantly improves the connection capacity. However, sufficient concrete depth underneath the socket should be secured to avoid the reduction of the capacity due to stress concentration at the bottom corners of the socket.
3. The connection behaviour is significantly affected by the volume of concrete around the socket which offers side confinement to the pocket. The proper side confinement by increasing the beam overhanging or beam width can enhance the capacity and control the propagation of cracks around the pocket corners.
4. To prevent premature failure in socket connections, design considerations should include a minimum socket depth of 1.4 times the column thickness, a minimum depth underneath the socket of 0.5 times the column thickness, an overhanging length of not less than 0.8 times the column thickness, and a ratio between the column width to the beam width of not less than 2.
5. Socket-filling material has a direct impact on the connection performance. Connections filled with ordinary concrete or epoxy resin achieved approximately similar capacities, while connections filled with UHPC allowed for achieving the same capacity with a 16% shallower socket depth.
6. The strength and stiffness of GFRP-RC precast socket connections significantly improved by increasing the amount of column longitudinal reinforcement at the connection region.

CRediT authorship contribution statement

El-Naqeeb Mohamed H.: Writing – original draft, Validation, Software, Methodology, Formal analysis. **Hassanli Reza:** Writing – review & editing, Supervision, Project administration, Conceptualization. **Zhuge Yan:** Writing – review & editing. **Ma Xing:** Writing – review & editing. **Manalo Allan:** Writing – review & editing.

Declaration of Competing Interest

The authors declare that they have no known competing financial interests or personal relationships that could have appeared to influence the work reported in this paper.

Data availability

Data will be made available on request.

References

[1] Culmo M.P., Lord B., Huie M., Beerman B. Accelerated bridge construction: experience in design, fabrication and erection of prefabricated bridge elements and systems: final manual. United States. Federal Highway Administration. Office of Bridge Technology; 2011.
[2] Elliott K.S. Precast concrete structures: Crc Press; 2019.
[3] Zheng G, Kuang Z, Xiao J, Pan Z. Mechanical performance for defective and repaired grouted sleeve connections under uniaxial and cyclic loadings. Constr Build Mater 2020;233:117233.
[4] Wang Z, Wu C, Li T, Xiao W, Wei H, Qu H. Experimental study on the seismic performance of improved grouted corrugated duct connection (GCDC) design for precast concrete bridge column. J Earthq Eng 2022;26:2469–90.
[5] Wang Z, Li T, Qu H, Wei H, Li Y. Seismic performance of precast bridge columns with socket and pocket connections based on quasi-static cyclic tests: experimental and numerical study. J Bridge Eng 2019;24:04019105.
[6] Cheng Z, Sritharan S. Side shear strength of preformed socket connections suitable for vertical precast members. J Bridge Eng 2019;24:04019025.
[7] Piras S, Palermo A, Saiid Saiidi M. State-of-the-art of posttensioned rocking bridge substructure systems. J Bridge Eng 2022;27:03122001.
[8] Liu Y, Li X, Zheng X, Song Z. Experimental study on seismic response of precast bridge piers with double-grouted sleeve connections. Eng Struct 2020;221:111023.
[9] Yan Q, Chen T, Xie Z. Seismic experimental study on a precast concrete beam-column connection with grout sleeves. Eng Struct 2018;155:330–44.
[10] Haraldsson OS, Janes TM, Eberhard MO, Stanton JF. Seismic resistance of socket connection between footing and precast column. J Bridge Eng 2013;18(9):910.
[11] Han Y, Dong J, Wang L. Experimental study on the seismic performance of socket bridge piers. Adv Civ Eng 2020;2020:1–10.
[12] Zhang G, Han Q, Xu K, Du X, He W. Experimental investigation of seismic behavior of UHPC-filled socket precast bridge column-foundation connection with shear keys. Eng Struct 2021;228:111527.
[13] Mehrsoroush A, Saiidi MS. Cyclic response of precast bridge piers with novel column-base pipe pins and pocket cap beam connections. J Bridge Eng 2016;21:04015080.
[14] Cheng Z, Sritharan S. Outdoor test of a prefabricated column–pile cap–pile system under combined vertical and lateral loads. J Bridge Eng 2020;25:04020052.
[15] Zhou X, Nie X, Xu S, Ding R, Zhang C, Yin X. Experimental studies on seismic performance of socket connections with shear keys and inner and outer filled reinforced concrete. Eng Struct 2022;273:115021.
[16] Croce P, Formichi P, Landi F. Influence of reinforcing steel corrosion on life cycle reliability assessment of existing RC buildings. Buildings 2020;10:99.
[17] Cadenazzi T, Dotelli G, Rossini M, Nolan S, Nanni A. Cost and environmental analyses of reinforcement alternatives for a concrete bridge. Struct Infrastruct Eng 2020;16:787–802.
[18] Manalo A, Maranan G, Benmokrane B, Cousin P, Alajarmeh O, Ferdous W, et al. Comparative durability of GFRP composite reinforcing bars in concrete and in simulated concrete environments. Cem Concr Compos 2020;109:103564.

[19] Nanni A, De Luca A, Zadeh HJ. Reinforced concrete with FRP bars: Mechanics and design. CRC press; 2014.
[20] Ghomi SK, El-Salakawy E. Effect of joint shear stress on seismic behaviour of interior GFRP-RC beam-column joints. Eng Struct 2019;191:583–97.
[21] Mady M, El-Ragaby A, El-Salakawy E. Seismic behavior of beam-column joints reinforced with GFRP bars and stirrups. J Compos Constr 2011;15:875–86.
[22] Safdar M, Sheikh MN, Hadi MN. Finite element analysis to predict the cyclic performance of GFRP-RC exterior joints with diagonal bars. J Build Eng 2023;65:105774.
[23] Ngo TT, Pham TM, Hao H, Chen W, San HaN. Proposed new dry and hybrid concrete joints with GFRP bolts and GFRP reinforcement under cyclic loading: Testing and analysis. J Build Eng 2022;49:104033.
[24] Hassanli R, Vincent T, Manalo A, Smith ST, Gholampour A, Gravina R. Large-scale experimental study on pocket connections in GFRP-reinforced precast concrete frames. In: *Structures*. 34. Elsevier; 2021. p. 523–41.
[25] Hassanli R, Vincent T, Manalo A, Smith ST, Gholampour A, Gravina R, et al. Connections in GFRP reinforced precast concrete frames. Compos Struct 2021;276:114540.
[26] Ghanbari-Ghazijahani T, Hassanli R, Manalo A, Smith ST, Vincent T, Gravina R, et al. Cyclic behavior of beam–column pocket connections in GFRP-reinforced precast concrete assemblages. J Compos Constr 2023;27:04022107.
[27] ACI CODE-. 440.11–22: Building Code Requirements for Structural Concrete Reinforced with Glass Fiber-Reinforced Polymer (GFRP) Bars—Code and Commentary. American Concrete Institute; 2023.
[28] Documentation A. Simulia. Providence, Rhode Island 2022.
[29] El-Naqeeb MH, El-Metwally SE, Abdelwahed BS. Performance of exterior beam-column connections with innovative bar anchorage schemes: numerical investigation. Struct: Elsevier 2022:534–47.
[30] Cheng Z, Liu D, Li S, Wang J, Zhang J. Performance characterization and design recommendations of socket connections for precast columns. Eng Struct 2021;242:112537.
[31] Zhang G, Han Q, Xu K, Song Y, Li J, He W. Numerical analysis and design method of UHPC grouted RC column-footing socket joints. Eng Struct 2023;281:115755.
[32] El-Naqeeb MH, Abdelwahed BS, El-Metwally SE. Numerical investigation of RC exterior beam-column connection with different joint reinforcement detailing. Struct: Elsevier 2022:1570–81.
[33] Thorenfeldt E. Mechanical properties of high-strength concrete and applications in design. Symposium Proceedings, Utilization of High-Strength Concrete, Norway, 19871987.
[34] Wight JK, MacGregor JG. Reinforced concrete. UK: Pearson Education; 2016.
[35] Committee A. Building code requirements for structural concrete (ACI 318–19) and commentary. American Concrete Institute; 2019.
[36] Aslani F, Jowkarmeimandi R. Stress–strain model for concrete under cyclic loading. Mag Concr Res 2012;64:673–85.
[37] Genikomsou AS, Polak MA. Finite element analysis of punching shear of concrete slabs using damaged plasticity model in ABAQUS. Eng Struct 2015;98:38–48.
[38] El-Naqeeb MH, Abdelwahed BS. Nonlinear finite element investigations on different configurations of exterior beam-column connections with different concrete strengths in column and floor. Struct: Elsevier 2023:1809–26.
[39] Otoom OF, Lokuge W, Karunasena W, Manalo AC, Ozbakkaloglu T, Thambiratnam D. Experimental and numerical evaluation of the compression behaviour of GFRP-wrapped infill materials. Case Stud Constr Mater 2021;15:e00654.
[40] Mihu G., Mihalache I., Graur I., Ungureanu C., Bria V. Comparative study regarding friction coefficient for three epoxy resins. IOP Conference Series: Materials Science and Engineering: IOP Publishing; 2017. p. 012024.
[41] Gopal BA, Hejazi F, Hafezolghorani M, Yen Lei V. Numerical analysis and experimental testing of ultra-high performance fibre reinforced concrete keyed dry and epoxy joints in precast segmental bridge girders. Int J Adv Struct Eng 2019;11:463–72.
[42] Jin Z, Chen K, Pei S. Cyclic response of precast, hollow bridge columns with postpour section and socket connection. J Struct Eng 2022;148:06021005.